

Efficient Route for Cyclic Olefin Polymerization: Nonchelated Monodentate Benzimidazole Nickel(II) Complex Catalysts for Vinyl Polymerization of Norbornene

Naresh H. Tarte, Hyun Yong Cho, and Seong Ihl Woo*

Department of Chemical and Biomolecular Engineering (BK21 graduate program) & Center for Ultramicrochemical Process System (CUPS) and Department of Chemistry, Korea Advanced Institute of Science and Technology, 373-1 Guseong-dong, Yuseong-gu, Daejeon 305-701, Republic of Korea

Received July 30, 2007; Revised Manuscript Received August 28, 2007

ABSTRACT: We developed a series of nonchelated monodentate benzimidazole nickel complexes, bis[2-(2,6-difluorophenyl)-1*H*-benzimidazole]nickel(II) dibromide (**1**), bis[1-(2,6-difluorobenzyl)-2-(2,6-difluorophenyl)-1*H*-benzimidazole]nickel(II) dibromide (**2**), bis[2-methyl-1*H*-benzimidazole]nickel(II) dibromide (**3**), and bis[1-(2-methoxybenzyl)-2-(2-methoxyphenyl)-1*H*-benzimidazole]nickel(II) dibromide (**4**), upon activation with methylaluminoxane (MAO), which are found to be highly active for vinyl polymerization of norbornene (Nb). The polymerization activity displayed by **4** is as high as 1.68×10^9 g of PNB \cdot mol $_{\text{Ni}}^{-1}\cdot\text{h}^{-1}$ at very high Nb/Ni ratio of 1×10^5 . Moreover a small amount of MAO is required to achieve such activity with high yield. The comparable high activity of 4.96×10^8 g of PNB \cdot mol $_{\text{Ni}}^{-1}\cdot\text{h}^{-1}$ for the simplest complex **3** reveals the significance of nonchelation in this catalyst series. It is observed that the use of toluene as solvent inhibits the catalytic activity strongly. The in situ NMR analyses indicate that the ligand is still intact with the active species and hence the difference in activity is indeed being associated with the change in ligand.

Introduction

The major share of homogeneous catalysts applied by industry is based on trivalent monodentate phosphorus ligands,¹ but the uses of monodentate oxygen, nitrogen and sulfur ligands have been relatively overlooked. In the case of nitrogen, the bidentate chelates N \wedge N, N \wedge O, N \wedge S, and N \wedge P with imine nitrogen coordination are extensively used in polymerization² and other homogeneous transformations;³ to the best of our knowledge, the catalytic use of well-defined monodentate imine nitrogen coordination is highly limited.⁴ For few decades, ML₂X₂-type late transition metal complexes of biologically important monodentate benzimidazole have been reported,⁵ but they rarely have been used as a catalyst. Only one reference^{4a} is available for its use as catalyst for ethylene oligomerization. Recently proposed polymerization catalysts^{6,7} involve chelated benzimidazole ligands, which turned our attention toward monodentate benzimidazole as a potential imine nitrogen coordination ligand.

Polymerization of most of cyclic olefins shows low activities that may be attributed to slow insertion, i.e., the propagation rate caused by the steric hindrance of the bulky monomers. Kim et al.,⁸ on the basis of theoretical study, observed that the cyclopentyl group of norbornene, instead of acting as a steric barrier for insertion reaction, provides additional agostic sites and disposable ring strain. This is more effective on less sterically hindered catalysts. Similarly, Yoshida et al.,⁹ on the basis of coordination energy concept, observed higher reactivity of norbornene compared to ethylene toward the sterically open cationic metal center. Moreover, Woo et al.¹⁰ by density function theory (DFT) for ethylene insertion in zirconocene catalysts showed that the less congestive environment along with high electrophilic nature of the metal center results in tighter binding of ethylene to active center, which raises the transition state

energy and the same argument may apply in the case of norbornene.⁸ This leads us to develop monodentate benzimidazole coordination catalyst in a view to obtain less steric congestion for bulky cyclic olefins such as norbornene. The use of nickel makes the active center less electrophilic compared to high electrophilic early transition metal catalysts.

Vinyl polynorbornene is a specialty polymer which possesses interesting and unique properties such as high chemical resistance, high glass transition temperature, good ultraviolet resistance, low dielectric constant, excellent transparency, large refractive index, and low birefringence. As a result, in recent years, there have been considerable efforts for the development of “post-metallocene” catalysts for the vinyl polymerization of norbornene. An important contribution to the field is made by Rhodes, Goodall, Sen and co-workers¹¹ where as Janiak et al.¹² proposed a series of highly active nickel and palladium catalysts for homopolymerization of norbornene. We describe herein the catalytic performance of nonchelated nickel catalysts for vinyl polymerization of norbornene.

Experimental Section

General Considerations. All procedures were carried out by using standard Schlenk techniques. 1,2-dichlorobenzene (anhydrous grade), and nickel(II) bromide ethylene glycol dimethyl ether complex (97%) were purchased from Aldrich and was used without any further purification. Methylaluminoxane (MAO; Aldrich) was obtained as 10 wt % solutions in toluene and used without any further treatment. 2-methylbenzimidazole was purchased from Fluka (98%). Norbornene (bicyclo[2.2.1]hept-2-ene; Aldrich) was purified by distillation over potassium and was used as a solution in *o*-DCB just prior to polymerization.

Measurement. NMR spectra of ligands were recorded using CDCl₃ and DMSO-*d*₆ as solvents on a Bruker BMX-500 MHz instrument with tetramethylsilane (TMS) as the internal standard. The NMR analyses of active species were recorded using 2,6-dichlorobenzene-*d*₄ under dry argon. The ¹H NMR data of polynorbornene were recorded at ambient temperature and the ¹³C NMR

* Corresponding author. E-mail: siwoo@kaist.ac.kr. Korea Advanced Institute of Science and Technology (KAIST). Telephone: 82-42-869-3918. Fax: 82-42-869-8890.

Table 1. Vinyl Polymerization of Norbornene by Nickel/MAO^a

run	catalyst	norbornene (mmol)	MAO (mmol)	yields (g)	activity ^b	$M_w [\times 10^{-6}]$	M_w/M_n
1	1	12.8	0.9	0.92	7.36	5.17	2.8
2	1	20.0	0.9	1.05	8.40	4.53	2.8
3	1	30.0	0.9	1.15	9.20	5.35	2.7
4	1	20.0	1.5	1.40	9.58	5.06	2.7
5	1	20.0	2.4	0.98	6.85	5.08	2.9
6	2	12.8	0.9	0.94	7.52	3.32	2.7
7	2	20.0	0.9	1.11	8.88	4.37	2.6
8	2	30.0	0.9	1.32	10.5	4.38	2.6
9	2	20.0	1.5	1.18	9.44	3.59	3.1
10	2	20.0	2.4	0.87	6.96	3.87	3.2
11	3	12.8	0.9	0.62	4.96	3.56	3.6
12	4	12.8	0.9	1.1	8.80	3.32	2.8
13	4	20.0	0.9	1.48	11.8	3.56	3.6
14	4	30.0	0.9	1.82	14.5	3.94	3.6
15	4	30.0	1.5	2.11	16.8	4.39	3.1
16	4	30.0	2.4	1.70	13.6	4.63	2.7
17	4	30.0	3.0	1.54	12.3	3.72	2.6

^a Conditions: nickel precatalyst (0.3 μ mol); MAO 10 wt % solution in toluene; temperature, ambient, solvent, *o*-DCB (10.0 mL); t_p = 15 s; total volume = 15 mL. ^b Activity in 10^8 g of PNB \cdot mol $_{Ni}^{-1}$ ·h $^{-1}$.

data was recorded at 100 °C using 2,6-dichlorobenzene-*d*₄ as solvent on a Bruker AMX-500 MHz spectrometer. The FTIR analyses of complexes **1–4** and polynorbornene produced by **1–4** were studied by ATR–FTIR spectrometer (Sens IR). The combined differential scanning calorimeter–thermogravimetric analysis (DSC–TGA) was studied under nitrogen by Setsys 16/18 (SETRAM) instrument and the DSC data was studied under nitrogen up to 500 °C with a heating rate of 10 °C/min by NETZSCH DSC-204F1. Molecular weight and molecular weight distribution of polynorbornene were measured by gel permeation chromatography (GPC) (PL-GPC 220) at 160 °C using 1,2,4-trichlorobenzene as solvent and calibrated by polystyrene standards. Elemental analysis was investigated by Faison's elemental analyzer-1110. The melting points of ligands and complexes were measured by electrical apparatus with Mettler Toledo FP90 Control Processor.

Syntheses. All the ligand and complex syntheses were carried out under nitrogen atmosphere.

Synthesis of 2-(2,6-Difluorophenyl)-1H-benzimidazole (DF–PBI). The 2,6-difluorobenzoyl chloride (1.94 g, 11.0 mmol) was dissolved in dichloromethane (20 mL), and was added dropwise over 1 h to a solution of 1,2-diaminobenzene (1.08 g, 10.0 mmol) and triethylamine (1.9 mL, 13.5 mmol) in dichloromethane (100 mL) at 0 °C. The reaction mixture was stirred at 0 °C for 1 h, then the temperature was set to room temperature while stirring continued over the next 3 h, the volatiles were removed in vacuum to produce a pale yellow solid. The solid was dissolved in glacial acetic acid (50 mL), sodium acetate (0.90 g, 11.0 mmol) was added, and the mixture was refluxed for 21 h. The reaction mixture was cooled to room temperature, evaporated in vacuum, and partitioned between dichloromethane and water. The biphasic mixture was cooled in an ice bath, and neutralized with solid potassium carbonate with vigorous stirring. The phases were separated, and the extraction was completed with additional portions of dichloromethane. The combined organic extracts were dried with Na₂SO₄, and evaporated in vacuum. Purification by column chromatography (silica gel, *n*-hexane/ethyl acetate, 10/1) produced the DF–PBI compound (1.9 g, 82%) as a white solid. Melting point 202 °C; ¹H NMR (500 MHz, CDCl₃): δ 10.16 (br, 1H), 7.90 (br, 2H), 7.50 (m, 1H), 7.39–7.31 (m, 2H), 7.06 (m, 2H). ¹³C NMR (500 MHz, DMSO-*d*₆): δ 109, 112, 118, 122, 132–134, 141–143, 159, 161 ppm.

Synthesis of 1-(2,6-Difluorobenzyl)-2-(2,6-difluorophenyl)-1H-1,3-benzimidazole (DF–BPBI). To the solution of 1,2-diaminobenzene (1.08 g, 10.0 mmol) and stoichiometric sodium acetate in glacial acetic acid (30 mL) was added dropwise 2,6-difluorobenzaldehyde (2.98 g, 21.0 mmol) in glacial acetic acid (50 mL). After complete addition at room temperature, the resultant mixture was set to reflux for 21 h. Further treatment similar to (DF–PBI), gave the title compound in 54% (1.92 g) yield along with 21% (0.48 g) DF–PBI. Melting point: 145 °C. ¹H NMR (500 MHz, CDCl₃): δ 7.84 (m, 1H), 7.50 (m, 1H), 7.48 (m, 1H), 7.29 (m, 2H), 7.21 (m, 1H), 7.06 (m, 2H), 6.80 (m, 2H), 5.36 (s, 2H). ¹³C NMR (500 MHz, CDCl₃): δ 143.2, 143.1, 134.7, 132.3, 130.7, 130.6, 123.4, 122.5.

Synthesis of 1-(2-Methoxybenzyl)-2-(2-methoxyphenyl)-1H-1,3-benzimidazole (MO–BPBI). The MO–BPBI was synthesized in 75% (2.58 g) yield from 1,2-diaminobenzene (1.08 g, 10.0 mmol) and *o*-anisaldehyde (2.86 g, 21.0 mmol) by a method to that used for preparing DF–BPBI. Melting point: 151 °C; ¹H NMR (500 MHz, CDCl₃): δ 7.84 (d, 1H); 7.53 (m, 1H); 7.51 (m, 1H); 7.25–7.17 (m, 4H); 7.03 (t, 1H); 6.93 (d, 1H); 6.81 (d, 1H); 6.75 (t, 1H); 6.69 (dd, 1H); 5.23 (s, 2H); 3.76 (s, 3H); 3.56 (s, 3H). ¹³C NMR (500 MHz, CDCl₃): δ 157.6, 156.5, 143.3, 135.5, 132.4, 131.4, 128.4, 127.7, 124.5, 122.5, 121.9, 120.8, 120.4, 119.8, 119.8, 110.9, 110.6, 109.9, 55.1, 55.2, 55.1, 43.5 ppm.

Synthesis of Bis[2-(2,6-difluorophenyl)-1H-benzimidazole]nickel(II) Dibromide (1). A well-stirred solution of 0.51 g (2.2 mmol) of DF–PBI in anhydrous dichloromethane (10 mL) was added dropwise to a solution of nickel(II) bromide ethylene glycol dimethyl ether complex (0.31 g, 1.0 mmol) in anhydrous dichloromethane (20 mL), under inert atmosphere. A color change from faint orange to a deep blue was observed which yield blue precipitate after stirring for next 6 h at room temperature and filtered through a glass filter and the filtrate was evaporated in vacuo to yield the title complex as blue solid. Dark blue crystals were obtained in acetonitrile. Yield: 76% (0.52 g). Anal. Calcd for C₂₆H₁₆Br₂F₄N₄Ni: C, 46.00; H, 2.38; N, 8.25. Found: C, 45.92; H, 2.43; N, 8.36.

Synthesis of Bis[1-(2,6-difluorobenzyl)-2-(2,6-difluorophenyl)-1H-benzimidazole]nickel(II) Dibromide (2). A procedure similar to **1** was employed for the synthesis of the complexes **2–4**. A blue solid was yielded as the sole product in 72% (0.52 g) yield. Crystallized acetonitrile/acetone (1:1) binary solvent system. Melting point: 252 °C. Anal. Calcd for C₄₀H₂₄Br₂F₈N₄Ni: C, 51.60; H, 2.60; N, 6.02. Found: C, 51.83; H, 2.46; N, 6.04.

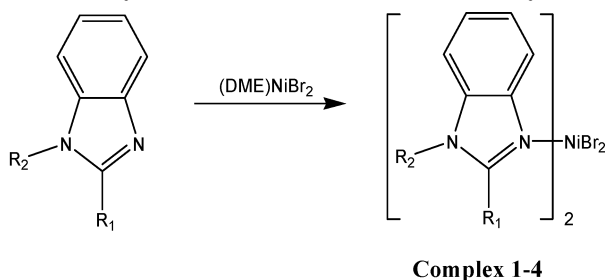
Synthesis of Bis[2-methyl-1H-benzimidazole]nickel(II) Dibromide (3). A violet crystalline solid was obtained in 65% (0.60 g) yield. Anal. Calcd for C₁₆H₁₆Br₂N₄Ni: C, 39.80, H, 3.34; N, 11.60. Found: C, 39.89; H, 3.30; N, 11.66.

Synthesis of Bis[1-(2-methoxybenzyl)-2-(2-methoxyphenyl)-1H-benzimidazole]nickel(II) Dibromide (4). A sky blue crystalline solid was obtained with 68% (0.33 g) yield. Melting point 289 °C. Anal. Calcd for C₄₄H₄₀Br₂N₄NiO₄: C, 58.25, H, 4.44; N, 6.18. Found: C, 58.27; H, 4.48; N, 6.47.

X-ray Crystallography. The X-ray structure analyses data were collected using a Bruker SMART Apex II X-ray diffractometer, and the structure solution and refinement were performed by using the SHELXS program.¹³

Polymerization of Norbornene. The polymerization runs were performed in 100 mL glass reactors using 2,6-dichlorobenzene (*o*-DCB) as the solvent at ambient temperatures. In a typical polymerization (run 12, Table 1), 0.3 μ mol of precatalyst **4** was dissolved in *o*-DCB (11.0 mL) under nitrogen atmosphere, and 12.8 mmol (2.7 mL) solution of norbornene in *o*-DCB was added. The polymerization was initiated by adding a toluene solution of MAO

Scheme 1. Synthetic Routes for Nonchelated Precatalysts 1–4



Complex 1. R_1 = 2,6-difluorophenyl, R_2 = H

Complex 2. R_1 = 2,6-difluorophenyl, R_2 = 2,6-difluorobenzyl

Complex 3. R_1 = CH₃, R_2 = H

Complex 4. R_1 = 2-methoxyphenyl, R_2 = 2-methoxybenzyl

(0.6 mL, 0.9 mmol). The highly viscous mass of polymer was observed immediately after the MAO addition. The polymerization was terminated within 15 s by adding acidified methanol (20 mL, 5% HCl). The polymer was isolated by filtration, washed with methanol and dried in vacuum at 100 °C for 24 h. Unless otherwise stated, the total volume was 15 mL, which was achieved by variation of amount of *o*-DCB when necessary. All the polymers were characterized by IR and NMR and were found exclusively to be vinyl-type polynorbornene.

Results and Discussion

Synthesis of Precatalysts 1–4. The monodentate ligands used in this study are 2-(2,6-difluorophenyl)-1*H*-benzimidazole (DF–PBI), 1-(2,6-difluorobenzyl)-2-(2,6-difluorophenyl)-1*H*-benzimidazole (DF–BPBI), 2-methyl-1*H*-benzimidazole (M–BI) and 1-(2-methoxybenzyl)-2-(2-methoxyphenyl)-1*H*-benzimidazole (MO–BPBI). The synthesis and biological activities of these aryl-substituted benzimidazole ligands are well documented.^{14a,14b} The DF–PBI ligand similar to its analogous^{14c} can be easily prepared by reacting 2,6-difluorobenzyl chloride with 1,2-diaminobenzene in high yield. The benzyl substituted ligands (DF–BPBI and MO–BPBI) were prepared using thermal procedure,^{14d} by refluxing a proper benzaldehyde with 1,2-diaminobenzene. The neutral precatalysts [Ni(DF–PBI)₂Br₂] (1), [Ni(DF–BPBI)₂Br₂] (2), [Ni(M–BI)₂Br₂] (3), and [Ni(MO–BPBI)₂Br₂] (4) were prepared by the reaction of dibromide nickel precursor with the corresponding benzimidazole in stoichiometric proportion (Scheme 1).

Structural Features of Precatalysts 1–4. We developed precatalyst 1 with phenyl substitution on benzimidazole carbon and precatalyst 2 with phenyl substitution on benzimidazole carbon and benzyl substitution on amido benzimidazole nitrogen. Additionally, we synthesized precatalyst 3 without both the phenyl and benzyl substitution in benzimidazole, in order to see the steric and electronic contribution, if any, from the benzyl and phenyl substitution on polymerization performance. The coordination of the alkoxy oxygen to the neutral nickel(II) center where the norbornene vinyl polymerization activity increases with bulkiness of the alkoxy group has been reported.¹⁵ Such coordination by methoxy oxygen was not observed in the case of complex 4 (Figure 1), which we developed in order to see any effect from the heteroatom. All these complexes are diimine-type with a pseudotetrahedral geometry. These complexes are found to be stable at high temperature. The TGA analyses shows that the first onset decomposition temperature is 331, 335, and 280 °C for complexes 1–3 which are higher than those reported for cobalt and copper complexes.^{4a} The complex 4 shows first

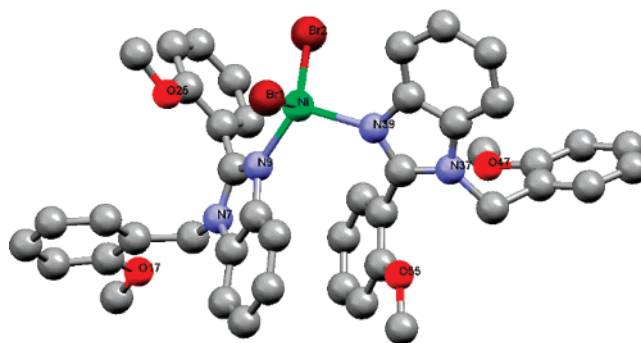


Figure 1. X-ray structure of complex 4 along with selected bond lengths (Å) and angles (deg). Hydrogen atoms are omitted for clarity: Ni–N(9) 1.993, Ni–N(39) 2.028, Ni–Br(1) 2.3900, Ni–Br(2) 2.3651; N(9)–Ni–N(39) 108.4, N(9)–Ni–Br(1) 103.57, N(9)–Ni–Br(2) 115.49, N(39)–Ni–Br(1) 104.01, N(39)–Ni–Br(2) 100.21, Br(1)–Ni–Br(2) 123.80.

onset decomposition at 190 °C, which is the lowest among the series.

Vinyl Polymerization of Norbornene Using Precatalysts 1–4. In an attempt to homopolymerize norbornene using a high-throughput screening technique as reported by Cho et al.,¹⁶ we observed catalyst 1/MAO to be highly active, producing exclusively vinyl-type polynorbornene. The exceptionally high activity of catalyst 1/MAO (Table 1) enabled us to establish tentatively the precatalyst structure activity correlation and investigate the factors which originate such an extremely high activity. The addition of MAO to the precatalyst/norbornene solution immediately turned to a highly viscous mass which was unable to stir further even for very high norbornene to nickel ratio (1×10^5) and hence a short period of 15 s polymerization experiments were carried. Stop-flow polymerization technique¹⁷ has been successfully applied for a very short period polymerization and the present system can be an efficient candidate for such technique.

Effect of Precatalyst Structure on Polymerization Performance. The catalytic trials (Table 1) show that upon activation with MAO, all the catalysts are extremely active for vinyl polymerization of norbornene. Similar to late-transition metal complexes as catalysts for ethylene polymerization,¹⁸ the electronic and steric effects of individual ligands affect the catalytic performance and the molecular mass of the resultant polynorbornene. In the case of precatalysts 1 (runs 1–5) and 2 (runs 6–10), the activity is not affected considerably but the molecular weight decreased almost by one-third for precatalyst 2. Such resemblance of molecular weight can also be seen for precatalysts 1 and 4. In addition, comparing the performance of precatalysts 1 (runs 1–5) and 3 (run 11); the absence of the phenyl group in 3 decreased not only the activity almost by one-third but also the molecular weight. The lower catalytic performance of precatalyst 3 lies in its sterically and electronically poor nature. The decreased molecular weight for precatalysts 2 (runs 6–8), 3 (run 11), and 4 (runs 12–14), compared to precatalyst 1 (runs 1–3) indicates a higher rate of insertion/propagation for precatalyst 1.

Among the series, precatalyst 4 (runs 12–17) showed the highest activity for vinyl polymerization of norbornene. The maximum activity of 1.68×10^9 g of PNb·mol_{Ni}^{−1}·h^{−1} was reached with high (91%) conversion and very high norbornene to nickel ratio of 1×10^5 in a 15 s polymerization run (run 15). The activity of precatalyst 4 is higher than the activity reported for any catalytic system until date.^{12,19} It is interesting to note that similar high activity value for precatalyst 3 which is coordinated with a simple ligand having neither any electronic

nor steric substitution reveals the significance of nonchelation in this catalyst series. The DFT study¹⁰ for ethylene polymerization suggests that more open structure for these catalysts lowers the transition state barrier compared to less open structured catalysts. Hence the high activity of **1–4** is the combined result of a nonchelated and an open structure (N–Ni–N = 123.80° for **4** and 118.3° for **1**) around the nickel center, and for precatalyst **4** the additional contribution is from the heteroatom,²⁰ which can protect the active site and termination reaction.

In the case of norbornene/ethylene copolymerization,^{9,21} a very high rate of chain termination is observed in the sterically hindered catalysts. During the propagation step, norbornene forms crowded environment around the metal center which results in insertion of ethylene instead of norbornene followed by chain termination via β -hydride elimination. The high chain termination rate for bulky monomer such as norbornene can be avoided in the case of nonchelated catalysts which can easily insert the bulky norbornene to active nickel center due to nonchelated geometry, which is rather difficult in the case of the chelated complexes. It is noteworthy that this activity is related to the high turn over number of 4980 s⁻¹ which is being reminiscent of enzymic catalysis. It means that the insertion/propagation rate is very high which is due to the nonchelation bonding of metal with monodentate ligands which can adopt “lock and key” type geometry with incoming norbornene in transition state as observed in enzymatic catalysis.

Effect of Norbornene and MAO Concentration. The polymerization data confirms that increase in norbornene concentration increased the molecular weight. Hence chain transfer to norbornene did not occur, which is rather difficult due sterically hindered propagation chain end and the bulky norbornene monomer. Moreover due to the bicyclic structure of norbornene, one M–C–C–H unit of the LnM(polynorbornyl) species can not achieve the planar conformation that is normally required for β -H elimination, and the other contains bridgehead carbon, so that the β -H elimination would generate a bridgehead olefin, which is very unstable and hence unfavorable. After the first norbornene insertion, propagation ensues and molecular weights increases to very large values. Among the series, the highest molecular weight of value 5.35×10^6 g·mol⁻¹ with an activity of value 9.20×10^8 g of PNB·molNi⁻¹·h⁻¹ was observed for **1** (run 3). The molecular weight is one of the highest reported for homogeneous polymerization catalysts, which ultimately suggests that a very little chain termination occurs in polymerization carried out by **1**. Hence a little chain termination to aluminum was occurring in the polymerization carried by this catalyst system. Moreover, the rate of polymerization increases with norbornene concentration but does not increased by first order with respect to the norbornene concentration, which suggests that the monomer diffusion through reaction medium to the active center can most probably be the rate-determining step in this catalyst system.

The high activity catalysts reported earlier are hampered by the high amount of MAO necessary for activation. It is still necessary to have a low MAO concentration to reduce industrial operating costs and the amount of cocatalyst residues in the polymer, which are more advantages for the prospective optical applications of polynorbornene.^{12a,b} The activation of all the precatalysts **1–4**, requires optimal MAO concentration of 1.5 mmol (Al/Ni = 5000) which generates maximum active sites as seen from its highest activity. This MAO concentration is 6-fold less than the high active catalyst reported for vinyl polymerization of norbornene.^{19a} A further increase in the MAO

Table 2. Temperature and Toluene Effect on Norbornene Polymerization by 4/MAO^a

run	catalyst	temp (°C)	solvent	yields (g)	activity ^b	M_w [$\times 10^{-6}$]	M_w/M_n
1	4	0	<i>o</i> -DCB	1.30	10.4	5.47	3.3
2	4	60	<i>o</i> -DCB	1.15	9.20	3.04	2.3
3	4	80	<i>o</i> -DCB	0.99	7.92	2.42	2.5
4 ^c	4	25	<i>o</i> -DCB:Tol	0.41	0.08	1.30	2.6
5 ^d	4	25	<i>o</i> -DCB:Tol	0.14	0.03	0.48	2.5

^a Conditions: nickel precatalyst (0.3 μ mol); MAO (0.9 mmol) 10 wt % solution in toluene; norbornene (20 mmol); solvent, *o*-DCB; t_p = 15 s; total volume = 15 mL. ^b Activity in 10^8 g of PNB·molNi⁻¹·h⁻¹. ^c In 1:1 toluene/*o*-DCB, t_p = 10 min. ^d In 5:1 toluene/*o*-DCB, t_p = 10 min.

concentration decreased the activity and this could be explained on the basis of deactivating interaction of free trimethylaluminum present in MAO with the active complex.

Effect of Temperature and Toluene on Norbornene Polymerization by 4/MAO. Effect of change in polymerization temperature (Table 2) for precatalyst **4**, suggests that maximum activity can be achieved at 25 °C (Table 1, run 13), however highest molecular weight can be achieved at 0 °C (Table 2, run 1) which decrease with increase in temperature. The in situ NMR for 2/dMAO (Figure 3) shows that with increase in temperature the concentration of free TMA increased in the system. Hence similar increase of TMA with temperature in 4/MAO might have caused the activity fall at higher temperature. Alt et al. in the case of cobalt catalysts reported²² that very small amounts of toluene can strongly inhibit the norbornene polymerization activity. We observed that in the case of 4/MAO the polymerization activity in *o*-DCB/toluene dropped drastically, which proves the strong inhibition effect of toluene in this system too. The probable reason may be the formation of tight or contact ion pair of the active species in nonpolar solvent as the solvated ion pair formation is dominant in polar solvent. However it will not be realistic to assert that such high activity is originated due to solvent effect of *o*-DCB, as reports are available for low activity catalysts in highly polar solvents, and hence, there is a significant contribution from nonchelation.

Nature of Active Species. Similar to metallocene catalysts,²³ late transition metal catalysts also show cation-like species in polymerization system. Talsi et al.²⁴ observed that upon activation with high excess MAO (Al/metal > 500) “cation-like” species, [LFe(μ -Me)₂AlMe₂]⁺[Me–MAO]⁻ (L = bis(imino)-pyridine ligand) was dominant in polymerization system during ethylene polymerization by iron/MAO systems. Recent theoretical study by Zurek et al.^{23e} also supports such ion pair dominance. In the case of catalysts **1–4**/MAO, the fairly narrow molecular weight distribution (M_w/M_n = 2.5–3.1), comparable catalytic performance, and the similar catalytic behavior toward MAO and norbornene concentration reveal that upon activation with MAO, a common type of active species is generated in this series. During the in situ NMR study for activation of precatalyst **2** with dMAO, we observed that the addition of dMAO to the precatalyst **2** in deuterated *o*-DCB changed the color from light blue to clear dark brown, indicating the formation of active species. The ¹H NMR of 2/dMAO at Al/Ni-800 is shown in Figure 2 recorded at different time intervals. The spectra show that the ligand is an integral part of active species, moreover the active species is long-lived and formed polynorbornene upon addition of norbornene solution in *o*-DCB. Hence the difference in activity is indeed being associated with the change in ligand. The shoulder peak to MAO at -0.6 ppm which is assigned as μ -Me peak by Talsi and co-workers^{23f} in the case of zirconocene catalysts can also be seen. The variable temperature ¹H NMR of 2/dMAO at Al/Ni-200 (Figure 3) show

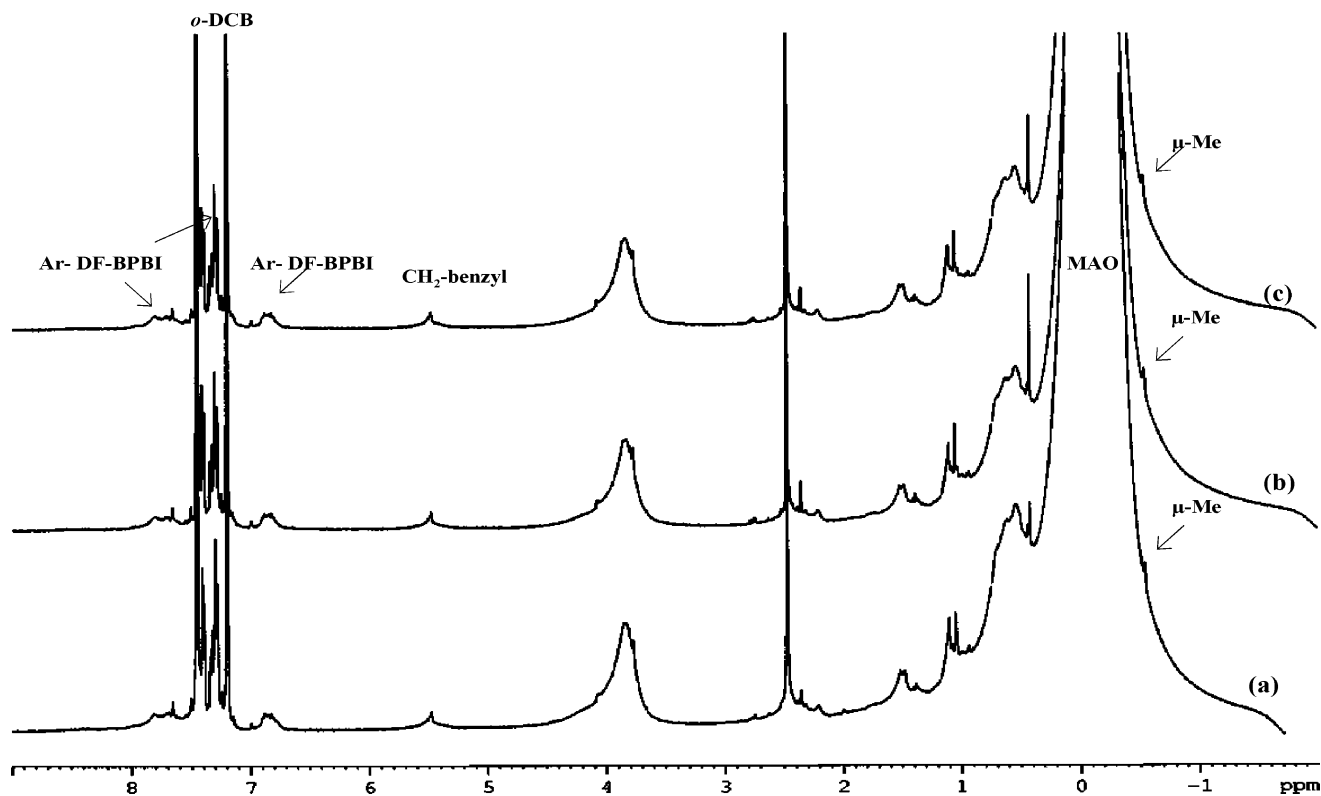


Figure 2. ^1H NMR analyses of 2/dMAO (Al/Ni-800) in $o\text{-DCB-}d_4$: (a) within 2 h; (b) after 1 week; (c) after 4 weeks.

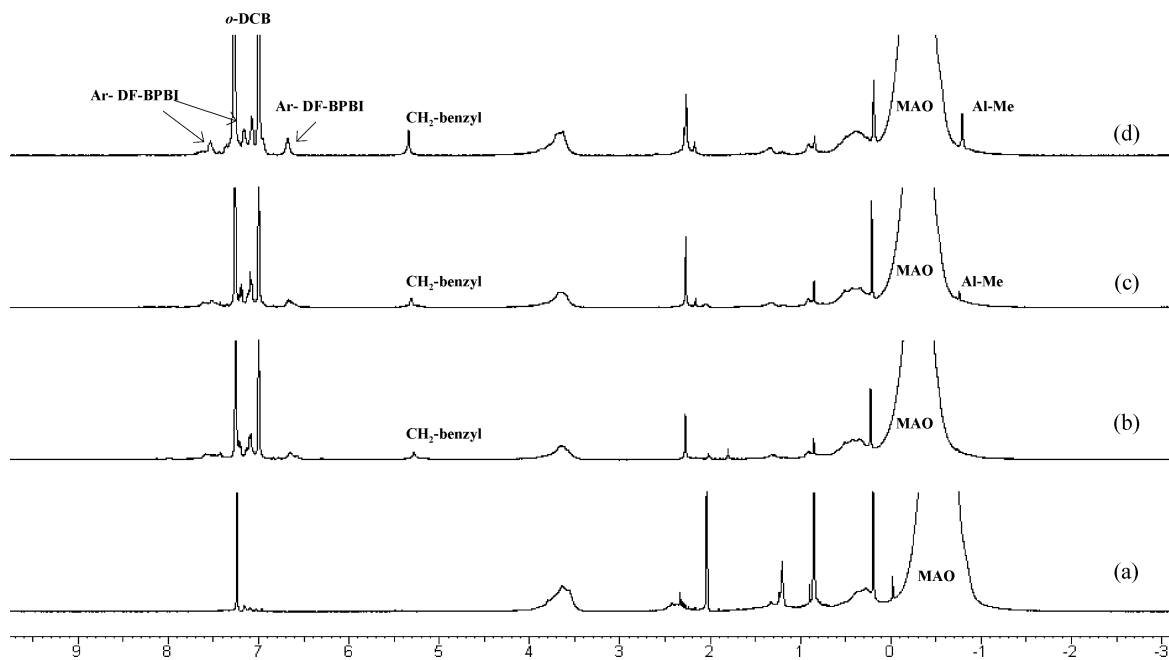


Figure 3. ^1H NMR analyses of 2/dMAO (Al/Ni-200) in $o\text{-DCB-}d_4$: (a) dMAO in CDCl_3 at 25 $^\circ\text{C}$; (b) 2/dMAO at 25 $^\circ\text{C}$; (c) 2/dMAO at 50 $^\circ\text{C}$; (d) 2/dMAO at 100 $^\circ\text{C}$.

neither $\mu\text{-Me}$ peak nor the free TMA peak at 25 $^\circ\text{C}$ which indicate that at lower Al/Ni cationic Ni/MAO anion pair like $[\text{L}_2\text{Ni}^\text{II}(\mu\text{-Me})(\mu\text{-Cl})\text{AlMe}_2]^+[\text{Me-MAO}]^-$ is formed. It is observed that with increase in temperature a new peak appear at -0.79 ppm and is assigned as free TMA peak, which might have caused the deactivation of active species, resulting in decrease of polymerization activity at increased temperature. Hence it is reasonable to conclude that a cationic Ni/MAO anion pair like $[\text{L}_2\text{Ni}^\text{II}(\mu\text{-Me})(\mu\text{-Cl})\text{AlMe}_2]^+[\text{Me-MAO}]^-$ is formed at Al/Ni-200 and the $[\text{L}_2\text{Ni}(\mu\text{-Me})_2\text{AlMe}_2]^+[\text{Me-MAO}]^-$ species is formed at Al/Ni-800 in **1–4** upon activation of MAO in

$o\text{-DCB}$ and the high activity is the result of an open and nonchelated structure of the active species.

Polynorbornene Characteristics. Attempts have been made to establish the polymer microstructure on the basis of earlier reports^{12,19,25} and the spectroscopic analyses for **1–4**, which confirm the formation of vinyl-type polynorbornene. The IR bands at 730 and 960 cm^{-1} are attributed to the *cis* and *trans* forms of double bonds in ring opening metathesis polymerization and which are absent in IR spectra for polynorbornene obtained by catalysts **1–4**, and hence, no trace of ROMP was observed. Moreover the absence of any signal at 20–24 ppm in a ^{13}C

NMR spectrum strongly indicates *exo*-enchainment of the polynorbornene.^{25a} The microstructure of polynorbornene obtained using catalyst **4** can be described as low disyndiotactic in nature. These polymers are soluble in chlorinated aromatic solvents and are high-temperature sustainable. The high glass transition temperature (T_g) of value 461 °C was observed for polynorbornene obtained by catalyst **4**.

Conclusions

We introduced a novel route by applying nonchelated catalyst concept for cyclic olefin specifically norbornene vinyl polymerization. These nonchelated nickel catalysts are extremely active and the catalyst **4**/MAO is proved to be the most active catalysts for vinyl polymerization of norbornene which shows activity of value 1.68×10^9 g of PNB·mol_{Ni}⁻¹·h⁻¹ at relatively lower MAO concentration. The origin of high activity is the nonchelation structure of these catalysts where as a proper substitution on benzimidazole further enhances the activity and molecular weight. The in situ NMR analyses show that these catalysts are working like conventional single site polymerization catalysts. Research is in progress for the proper ligand design and development of catalysts for polymerization of polar monomers.

Acknowledgment. This research was funded by the Center for Ultramicrochemical Process Systems (CUPS) sponsored by KOSEF (2006). We thank Dr. Y.-D. Gong and Dr. C.-H. Kim, Korea Research Institute of Chemical Technology, for their fruitful discussion, suggestions, and technical support. We also thank Mr. Y. -H. Hwang, Dr. J. -W. Shin, Dr. M. A. Khan, and Mr. L. Cui for their technical assistance.

Supporting Information Available: Cif files giving crystallographic data for complexes **1** and **4** and the ligand M-BPBI, a table giving the crystallographic data for **1** and **4**, figures showing the molecular structure of **1** and M-BPBI, the FTIR analysis and the combined TGA-DSC analysis of complexes **1**–**4**, the FTIR, ¹H NMR and the DSC analyses of the polynorbornene produced by **1**–**4**/MAO, and ¹³C NMR analysis of polynorbornene produced by **4**/MAO. This material is available free of charge via the Internet at <http://pubs.acs.org>.

References and Notes

- (1) (a) Evans, D.; Osborn, J. A.; Wilkinson, G. *J. Chem. Soc. A* **1968**, 3133–3142. (b) Evans, D.; Yagupky, G.; Wilkinson, G. *J. Chem. Soc. A* **1968**, 2660–2665. (c) Brown, C. K.; Wilkinson, G. *J. Chem. Soc. A* **1970**, 2753–2764.
- (2) Ittel, S. D.; Johnson, L. K.; Brookhart, M. K. *Chem. Rev.* **2000**, *100*, 1169–1203.
- (3) Jacobsen, E. N.; Wu, M. H. In *Comprehensive Asymmetric Synthesis*; Jacobsen, E. N., Pfaltz, A., Yamamoto, H., Eds.; Springer: Berlin; 1999; p 649.
- (4) (a) Sun, W. H.; Shao, C.; Chen, Y.; Hu, H.; Sheldon, R. A.; Wang, H.; Leng, X.; Jin, X. *Organometallics* **2002**, *21*, 4350–4355. (b) Bennett, A. M. A.; Coughlin, E. B.; Donald, D. S.; Feldman, J.; Johnson, L. K.; Kreutzer, K. A.; McLain, S. J.; Nelson, L. T. J.; Parthasarathy, A.; Shen, X.; Tam, W.; Wang, Y. U.S. Patent 5,714,556, Feb. 3, 1998 to DuPont. (c) Li, K.; Darkwa, J.; Guzei, I. A.; Mapolie, S. F. *J. Organomet. Chem.* **2002**, *660*, 108–115.
- (5) (a) Goodgame, D. M. L.; Goodgame, M. *Inorg. Chem.* **1965**, *4*, 139–143. (b) Elder, M. S.; Melson, G. A.; Busch, D. H. *Inorg. Chem.* **1966**, *5*, 74–77. (c) Bose, K. S.; Patel, C. C. *J. Inorg. Nucl. Chem.* **1971**, *33*, 755–759. (d) Goodgame, M.; Cotton, F. A. *J. Am. Chem. Soc.* **1962**, *84*, 1543–1548.
- (6) (a) Tomov, A. K.; Chirinos, J. J.; Jones, D. J.; Long, R. J.; Gibson, V. C. *J. Am. Chem. Soc.* **2005**, *127*, 10166–10167. (b) Tomov, A. K.; Gibson, V. C.; Zaher, D.; Elsegood, M. R. J.; Daleb, S. H. *Chem. Commun.* **2004**, *17*, 1956–1957.
- (7) (a) Stibrany, R. T.; Schulz, D. N.; Kacker, S.; Patil, A. O. US Pat. 6,037,297, Mar. 14 2000 to Exxon Research and Engineering Co. and US Pat. 6,417,303 B1, Jul. 2000. (b) Stibrany, R. T. US Pat. 6,180,788 B1, Jan. 30, 2001 to Exxon Research and Engineering Company.
- (c) Patil, A. O.; Zushma, S.; Stibrany, R. T.; Rucker, S. P.; Wheeler, L. M. *J. Polym. Sci., Part A: Polym. Chem.* **2003**, *41*, 2095–2106.
- (8) Kim, E.-G.; Klein, M. L. *Organometallics* **2004**, *23*, 3319–3326.
- (9) (a) Yoshida, Y.; Nakano, T.; Tanaka, H.; Fujita, T. *Isr. J. Chem.* **2002**, *42*, 353–359. (b) Yoshida, Y.; Mohri, J.-I.; Ishii, S.-I.; Mitani, M.; Saito, J.; Matsui, S.; Makio, H.; Nakano, T.; Tanaka, H.; Onda, M.; Yamamoto, Y.; Mizuno, A.; Fujita, T. *J. Am. Chem. Soc.* **2004**, *126*, 12023–12032.
- (10) Woo, T. K.; Fan, J. L.; Ziegler, T. *Organometallics* **1994**, *13*, 2252–2261.
- (11) (a) Hennis, A. D.; Polley, J. D.; Long, G. S.; Sen, A.; Yandulov, D.; Lipian, J.; Benedikt, G. M.; Rhodes, L. F.; Huffman, J. *Organometallics* **2001**, *20*, 2802–2812. (b) Goodall, B. L.; McIntosh, L. H., III. US Pat. Appl. 0215735 A1, Sept. 29, 2005 to Rohm and Haas Company. (c) Bell, A.; Rhodes, L.; Goodall, B. L.; Fondran, J. C. WO Pat. 34344, June 15, 2000 to The B. F. Goodrich Company. (d) Lipian, J.-H.; Goodall, B. L.; Bell, A.; Mimna, R. A.; Fondran, J. C.; Hennis, A. D.; Polley, J. D.; Sen, A.; Jayaraman, S. WO Pat. 20472, April, 13, 2000 to the B. F. Goodrich Company. (e) McIntosh, L. H., III; Goodall, B. L.; Shick, R. A.; Jayaraman, S. WO Pat. 20871, June 12, 1997 to The B. F. Goodrich Company.
- (12) (a) Janiak, C.; Lassahn, P.-G. *Macromol. Rapid Commun.* **2001**, *22*, 479–492. (b) Berchtold, B.; Lozan, V.; Lassahn, P.-G.; Janiak, C. *J. Polym. Sci., Part A: Polym. Chem.* **2002**, *40*, 3604–3614. (c) Lassahn, P.-G.; Lozan, V.; Wu, B.; Weller, A. S.; Janiak, C. *Dalton Trans.* **2003**, 4437–4450. (d) Lassahn, P.-G.; Lozan, V.; Timco, G. A.; Christian, P.; Janiak, C.; Winpenny, R. E. P. *J. Catal.* **2004**, *222*, 260–267. (e) Janiak, C.; Lassahn, P.-G.; Lozan, V. *Macromol. Symp.* **2006**, *236*, 88–99.
- (13) (a) G. M. Sheldrick, SHELX-97, A Computer Program for Crystal Structure Solution and Refinement; Universitat Göttingen: Göttingen, Germany, 1997. (b) Sheldrick, G. (1990) SHELXTL-PC Release 4.1; Siemens Analytical X-ray Instruments, Inc.: Madison WI, 296pp.
- (14) (a) Roth, T.; Morningstar, M. L.; Boyer, P. L.; Hughes, S. H.; Buckheit, R. W., Jr.; Michejda, C. J. *J. Med. Chem.* **1997**, *40*, 4199–4207. (b) Perumal, S.; Mariappan, S.; Selvaraj, S. *ARKIVOC* **2004**, *8*, 46–51. (c) Fekner, T.; Gallucci, J.; Chan, M. K. *Org. Lett.* **2003**, *5*, 4795–4798. (d) Ladenburg, A. *Ber.* **1878**, *11*, 1648.
- (15) Lee, S. A.; Shin, K. Y.; Park, B. J.; Choi, M. K.; Lee, I.-M. *Bull. Korean Chem. Soc.* **2006**, *27*, 475–476.
- (16) Cho, H. Y.; Hong, D. S.; Jeong, D. W.; Gong, Y. D.; Woo, S. I. *Macromol. Rapid Commun.* **2004**, *25*, 302–306.
- (17) (a) Mori, H.; Saito, H.; Yamahiro, M.; Kono, H.; Terano, M. *Macromol. Chem. Phys.* **1998**, *199*, 613–618. (b) Mori, H.; Yamahiro, M.; Prokhorov, V. V.; Nitta, K.-H.; Terano, M. *Macromolecules* **1999**, *32*, 6008–6018. (c) Yamahiro, M.; Mori, H.; Nitta, K.-h.; Terano, M. *Macromol. Chem. Phys.* **1999**, *200*, 134–141. (d) Liu, B.; Matsuoka, H.; Terano, M. *Macromol. Rapid Commun.* **2001**, *22*, 1–24.
- (18) (a) Small, B. L.; Brookhart, M.; Bennett, A. M. A. *J. Am. Chem. Soc.* **1998**, *120*, 4049–4050. (b) Bruce, M.; Gibson, V. C.; Redshaw, C.; Solan, G. A.; White, A. J. P.; Williams, D. J. *Chem. Commun.* **1998**, 2523–2524. (c) Mecking, S. *Coord. Chem. Rev.* **2000**, *203*, 325–351.
- (19) (a) Sun, W.-H.; Yang, H.; Li, Z. *Organometallics* **2003**, *22*, 3678–3683. (b) Yang, H.; Sun, W.-H.; Chang, F.; Li, Y. *Appl. Catal., A* **2003**, *252*, 261–267.
- (20) Bianchini, C.; Mantovani, G.; Meli, A.; Migliacci, F.; Laschi, F. *Organometallics* **2003**, *22*, 2545–2547.
- (21) Benedikt, G. M.; Elce, E.; Goodall, B. L.; Kalamarides, H. A.; McIntosh, L. H., III; Rhodes, L. F.; Selvy, K. T.; Andes, C.; Oyler, K.; Sen, A. *Macromolecules* **2002**, *35*, 8978–8988.
- (22) Alt, F. P.; Heitz, W. *Macromol. Chem. Phys.* **1998**, *199*, 1951–1956.
- (23) (a) Bochmann, M.; Lancaster, S. *Angew. Chem., Int. Ed. Engl.* **1994**, *33*, 1634–637. (b) Babushkin, D. E.; Semikolenova, N. V.; Zakharov, V. A.; Talsi, E. P. *Macromol. Chem. Phys.* **2000**, *201*, 558–567. (c) Petros, R. A.; Norton, J. R. *Organometallics* **2004**, *23*, 5105–5107. (d) Bryliakov, K. P.; Talsi, E. P.; Bochmann, M. *Organometallics* **2004**, *23*, 149–52. (e) Zurek, E.; Ziegler, T. *Prog. Polym. Sci.* **2004**, *29*, 107–148. (f) Bryliakov, K. P.; Semikolenova, N. V.; Yudaev, D. V.; Zakharov, V. A.; Brintzinger, H. H.; Ystenes, M.; Rytter, E.; Talsi, E. P. *J. Orgmet. Chem.* **2003**, *683*, 92–102.
- (24) (a) Bryliakov, K. P.; Semikolenova, N. V.; Zakharov, V. A.; Talsi, E. P. *Organometallics* **2004**, *23*, 5375–5378. (b) Talsi, E. P.; Babushkin, D. E.; Semikolenova, N. V.; Zudin, V. N.; Panchenko, V. N.; Zakharov, V. A. *Macromol. Chem. Phys.* **2001**, *202*, 2046–2051.
- (25) (a) Kaminsky, W.; Bark, A.; Arndt, M. *Makromol. Chem. Macromol. Symp.* **1991**, *47*, 83–93. (b) Arndt, M.; Engelsen, R.; Kaminsky, W.; Zoumis, K. *J. Mol. Catal. A: Chem.* **1995**, *101*, 171–178. (c) Barnes, D. A.; Benedikt, G. M.; Goodall, B. L.; Huang, S. S.; Kalamarides, H. A.; Lenhard, S.; McIntosh, L. H., III; Selvy, K. T.; Shick, R. A.; Rhodes, L. F. *Macromolecules* **2003**, *36*, 2623–2632.